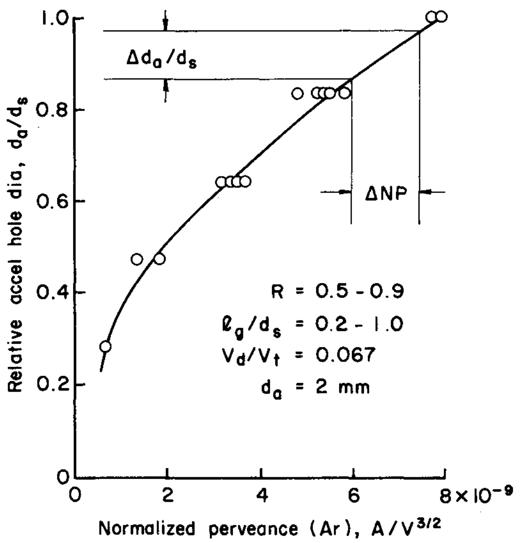

Fig. 2 Effect of accelerator hole diameter on maximum normalized perveance.

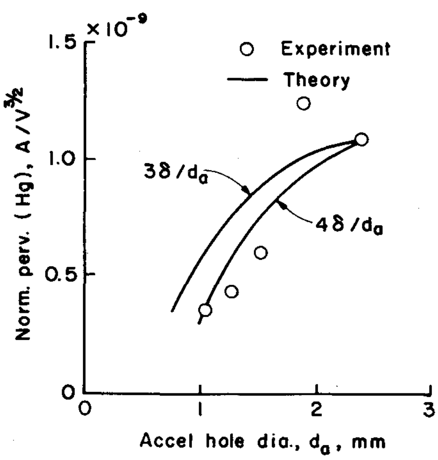

Fig. 3 Comparison of error theory with data from 30-cm thruster (Refs. 7 and 8).

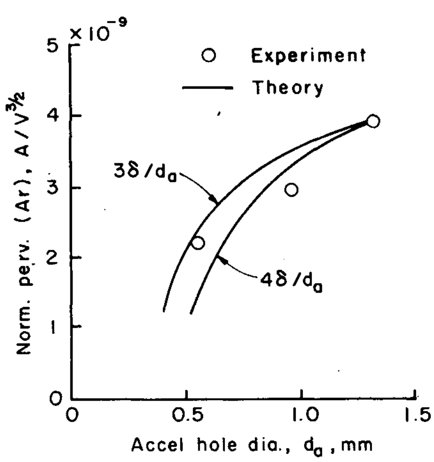

Fig. 4 Comparison of error theory with data ion-optics apparatus (Ref. 9).

should be smallest. Using the assumed accelerator displacement of 0.2 mm and the previously described effect of displacement on normalized perveance, the curves shown were produced. The upper curve was for a perveance change of $3\delta/d_a$, while the lower curve was for $4\delta/d_a$.

A similar approach was used for the data from the more recent ion optics study,[5] which are presented in Fig. 4. The maximum distance between supports in this study was only ~2 cm, so that the displacement due to relative thermal expansion could be ignored. The assumed alignment error was then only the initial value of 0.1 mm. Using this value and normalzing it to the data point for a d_s of 2.4 mm, the theory curves shown were produced.

Conclusions

The general trends of theory and experiment are similar. Because of the statistical nature of the problem, exact agreement should not, of course, be expected.

As stated earlier, there is no theoretical reason why smaller holes should have a decreased normalized perveance. The agreement between experiment and the error analysis presented herein indicates that past adverse effects of small ion-optics holes were due primarily to alignment errors. An obvious implication of this conclusion is that grids with smaller holes must be aligned with greater precision, if the full advantages of the smaller holes are to be realized.

The mounting techniques for the cited studies are, of course, not those used in current thrusters. Unfortunately, the visual/manual techniques used in these studies are still widely used for thrusters. The error associated with looking through a low-power magnifier and moving the grids by hand is therefore still present. A variety of mechanical jigging and alignment techniques will permit higher precision, and should be considered as replacements for what must now be considered an obsolete approach.

References

[1]Kaufman, H.R., and Robinson, R.S., "Electric Thruster Performance for Orbit Raising and Maneuvering," *Journal of Spacecraft and Rockets,* Vol. 21, March-April 1984, pp. 180-186.

[2]Kaufman, H.R., "Technology of Electron-Bombardment Ion Thrusters," in *Asvances in Electronics and Electron Physics,* Vol. 36, L. Marton, ed., Academic Press, New York, 1974, pp. 265-373.

[3]Rawlin, V.K., Banks, B.A., and Byers, D.C., "Dished Accelerator Grids on a 30-cm Ion Thruster," *Journal of Spacecraft and Rockets,* Vol. 10, Jan. 1973, pp. 29-35.

[4]Rawlin, V.K., "Studies of Dished Accelerator Grids for 30-cm Ion Thrusters," AIAA Paper No. 73-1086, Oct. 1973.

[5]Aston, G., Kaufman, H.R., and Wilbur, P.J., "Ion Beam Divergence Characteristics of Two-Grid Accelerator Systems," *AIAA Journal,* Vol. 16, May 1978, pp. 516-524.

[6]Kaufman, H.R., and Robinson, R.S., "Ion Source Design for Industrial Applications," *AIAA Journal,* Vol. 20, June 1982, pp. 745-760.

[7]Rovang, D.C. and Wilbur, P.J., "Ion Extraction Capabilities of Very Closely Spaced Grides," AIAA Paper No. 82-1894, Nov. 1982.

Thermal Control System of the Purdue University Space Shuttle Payload

John Aldrich Stark*
Purdue University, West Lafayette, Indiana

A REVIEW of the performance of the thermal control system used on the Purdue University Small Self-Contained Payload (SSCP) flown aboard STS-7 has been completed. During the design of this payload, severe

Received Jan. 13, 1984; revision submitted May 11, 1984.

*Graduate Student, School of Mechanical Engineering. Currently Engineer, Thermodynamics Technology, McDonnell Douglas Astronautics, St. Louis, Missouri. Associate Member AIAA.

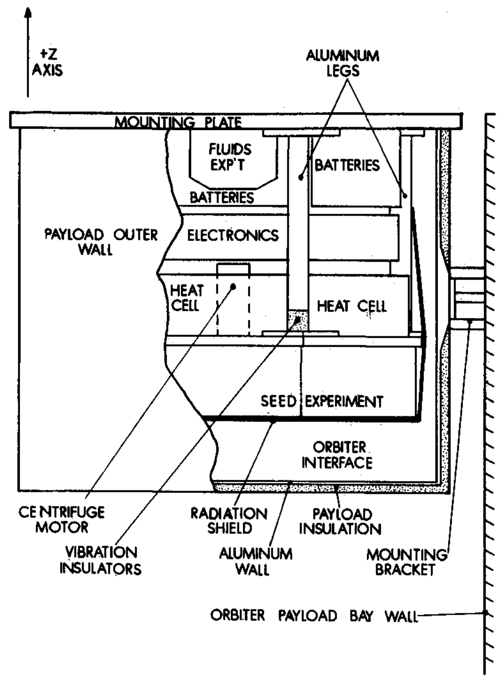

Fig. 1 Cutaway view of payload internal configuration.

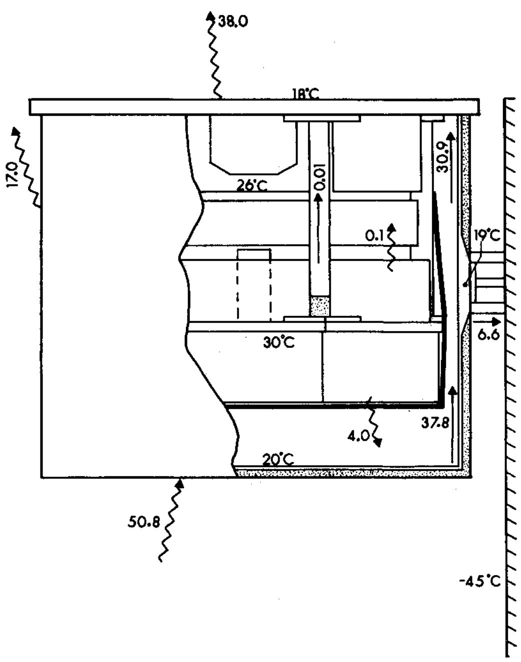

Fig. 2 Predicted heat flows. Zig-zag arrows represent net radiative transfers; straight arrows, conduction. All heat flows are in watts.

restrictions on certain operating temperatures necessitated a detailed analysis of the heat transfer processes involved and required the development of a suitable thermal control system. This paper reviews that analysis, describes the subsequent steps taken to control the temperatures, and comments on the in-flight performance of the system.

The payload was constrained to fit inside a 7.08-liter cylindrical container, 50.3 cm in diam by 36.2 cm high. The final mass was limited to 45.4 kg, and the entire space was to be self-contained. Self-containment meant that a large portion of the payload mass and volume had to be reserved for dry-cell batteries to power equipment. The payload consisted of three scientific experiments, three battery packs, and a microprocessor to control equipment and collect data. One of the experiments, a low-gravity seed-germination investigation, had a very limited range of allowable operating temperatures. Temperature restrictions on this experiment, and lesser ones on the microprocessor and batteries, defined the requirements for thermal control.

The heat transfer analysis was broken into four phases: Phase 1 included the prelaunch environment of the payload inside the orbiter; phase 2 extended from launch to 26 h into the flight, when the seed experiment was to begin; phase 3 encompassed the next 72 h, when the seed experiment would be running; and phase 4 was from termination of the seed experiment to Orbiter landing. The sequencing of experiments was to be executed by the microprocessor.

In the germination experiment, seeds were mounted on a centrifuge and housed in an aluminum canister. The centrifuge was to spin at a constant rate throughout the experiment, simulating a gravity field. The canister was filled with oxygen and nitrogen at 0.25 atm pressure. The seeds were to be maintained between 15 and 27°C during the experiment, and had no temperature requirements afterwards. Performance considerations allowed the battery packs to experience temperatures between 15 and 50°C prior to and during usage. The microprocessor was allowed a somewhat larger operating range.

Thermal protection provided with the payload canister included a conduction-resistant bracket which held the canister to the payload bay wall. Also provided was 0.795-cm-thick insulation (made of aluminized Kapton) surrounding the sides and bottom of the canister. Thus, these outer surfaces had a very low emissivity. A choice existed between two coatings for the outer surface of the mounting plate, which faced out of the bay. These coatings represented different ratios of emissivity/absorptivity. There was also an option of having insulation applied to the mounting plate.

The payload canister was mounted to the Orbiter's port side main longeron, which acts as the bay sill when the bay doors are open. For purposes of analysis, the canister top surface was considered to be level with the sill and perpendicular to the Orbiter $+z$ axis (which points "up" relative to the Orbiter). The canister was mounted slightly aft of the forward bay bulkhead. For simplicity, the payload outer surface was assumed to be gray and diffuse, as was the bay wall. Because of lack of prior knowledge of other payload geometries, locations, or times of residence in the bay, it was assumed that the bay was empty for all time. Approximation of a radiative view factor between the Purdue canister and the payload bay interior was then facilitated by numerical integration over both of these surfaces.

The flight plan for STS-7 involved several orbital maneuvers. A large part of the flight, however, was to be in an "Earth-viewing" attitude, in which the Orbiter $+z$ axis pointed toward the Earth's center. The magnitude of thermal radiation incident on the canister mounting plate in this attitude was determined to be approximately 605 W/m^2. This amount of energy was expected to provide mild internal temperatures for a payload without internal heat generation.[1]

Due to weight and cost limitations, it was decided that the temperature control system must be completely passive. After evaluating several possibilities, the configuration was finalized as follows. To provide passive, long-term temperature control under essentially steady-state conditions, the design incorporated three custom-built "heat cells." These cells were chosen because they contained a mixture of calcium chloride hexahydrate and Bisol II™ that melts at 27°C ($\Delta h_{fg} = 221$ kJ/kg), which was within the desired operating range of the seed experiment. They were rigidly mounted to the seed canister with a high-conductivity graphite paste. The heat cells would act as large heat sources/sinks (total capacity of 1585 kJ) as long as the phase-change material within was not completely liquid or solid. By using these heat cells, the final system configuration was made to be strongly dependent upon the anticipated preflight conditions within the Orbiter bay. That is, if the heat cells were warmer than 27°C prior to flight, they would be liquid and would act as heat sources during the flight. If cooler, they would act as heat sinks. It was determined that the heat cells would have a significantly higher temperature than 27°C for serveral days prior to launch. Therefore, the phase change material was assumed to be completely liquid at the time of launch.

Since the heat cell material was to begin in a liquid state, the design ideally would require a small net heat loss from the heat cells so that they would perform the function of a constant-temperature heat source throughout the experiment as they slowly converted back to the solid phase. However, it was not possible to adjust the heat balance to this condition. Instead, according to analysis, a small net heat gain would have to exist in the heat cells during the experiment. A viable situation was still possible, as there was to be a net heat loss in the 26 h of flight prior to commencement of the experiment, which would allow the heat cells to partially solidify. Then, during the experiment, net gains in the heat cells due to equipment heat generation would simply induce phase change back toward the liquid state. Predicted heat flow magnitudes and heat call states will be given later.

The internal heat balance was optimized with extensive use of a Fortran heat transfer simulation code. This program calculates heat transfer rates by assuming one-dimensional heat flows. The program provided less accuracy than desirable, but conformed to the available time schedule. Insulation was not used on the payload upper surface. The coating chosen for this surface was white paint ($\alpha_{solar} = 0.32$, $\epsilon = 0.94$). Figure 1 is a schematic of the arrangement of equipment within the canister. Because of the rubber vibration insulators, there was very little direct conduction expected between the seed canister and mounting plate. For purposes of combustion safety, a 0.1 atm nitrogen atmosphere was used external to the seed canister, which resulted in only limited convection/conduction. Therefore, the internal heat transfer problem was one primarily of radiation, although conduction through the gas was considered.

The remainder of the package was designed to incorporate minimal thermal interaction between any two components. Each surface was coated with paints or aluminum foil to enhance or inhibit the local radiation exchange as predicted to be necessary by the analysis program. The battery packs were mounted about 5 mm from the mounting plate, painted for high emissivity on the bottoms, and covered with bright aluminum foil on the outer sides to reduce radiation to the payload wall. Due to the large inner surface area of the payload canister wall, most of which directly viewed the seed experiment/heat cells, the primary loss of heat from the seed experiment/heat cells was by radiation to the payload inner wall. Therefore, a radiation shield of a thin fiberglass shell, covered on both sides with aluminum foil, was formed around the seed canister and along the sides of the internal hardware so that it surrounded all equipment except the battery packs and the fluids experiment (which were bolted directly to the mounting plate).

All pertinent heat transfer modes and temperatures are shown in Fig. 2. Values shown are those predicted by the analysis program for in-flight experiment conditions. These conditions include total heat generation (by batteries, centrifuge motor and electronics) of 8.7 W and a net heat storage rate in the heat cells of 0.66 W. Under the flight conditions with no equipment operating (no heat generation), the heat cells were predicted to change from 0% solid to 43% solid in the first 26 h (time from launch to beginning of seed experiment). Within the next 72 h, with all equipment running, the heat cells were predicted to change back to 32% solid due to the small net gain previously discussed. At that time the experiment would halt, and another 41 h would pass until the heat cells would become completely solid and begin to cool.

Post-flight investigation of the payload showed that the seed experiment was not activated as planned due to battery failure. However, the microprocessor was operative and able to collect data.

Due to communication problems, the microprocessor was not activated until 94 h into the flight. However, temperature measurements revealed that both the seed experiment and mounting plate experienced temperatures between 21 and 26°C from 94 to 145 h after launch. Note that no equipment was running at any time. Therefore, it appears that the initial heat cell loss rate was predicted slightly high. That is, the heat cells never completely solidified in 145 h, or if so, only shortly before the 145-h mark.

Though a detailed comparison between theoretical predictions and actual flight performance of the thermal control design can not be made, several things were learned. Most important was that where a passive system is necessary, a thermal storage device, such as the heat cells used here, appears to be a reliable and efficient method of controlling sensitive component temperatures. An alternate method would be to insulate (or shield) the payload or sensitive components heavily, which would occupy large volumes (and possibly present structural vibration problems in the case of radiation shields). Another possiblity explored here was designing for net heat loss of relatively large magnitude, and compensation with thermostat-controlled resistance heaters. This method may allow more precise control of temperatures, but would require excessive additional battery weight and volume. Also, the thermal inertia of a storage device can compensate readily for modeling errors by acting as either a sink or source to a large extent.

Acknowledgments

This work was partially funded by the NSF. The author expresses to his thanks to Dr. John T. Snow for advice, encouragement, and leadership, to Mr. Scott Flagg for manufacture of the heat cells, and to Dr. Harold Ritchie for donation of the payload canister.

References

[1] *Get Away Special Small Self-Contained Payloads Experimenter Handbook,* NASA Goddard Space Flight Center, Sounding Rocket Division, Greenbelt, Md., Oct. 1979.

[2] Touloukian, Y.S. ed., *Thermophysical Properties of Matter—TPRC Data Series,* Vols. 1, 2, 7, and 9, IFI/Plenum, New York, 1970.